ARTICLE

Sub-second heat inactivation of coronavirus using a betacoronavirus model

Yuqian Jiang[1] 🔬 | Han Zhang[1] | Jose A. Wippold[2] | Jyotsana Gupta[3] | Jing Dai[1] | Paul de Figueiredo[3] | Julian L. Leibowitz[3] | Arum Han[1,2]

[1]Department of Electrical and Computer Engineering, Texas A&M University, College Station, Texas, USA

[2]Department of Biomedical Engineering, Texas A&M University, College Station, Texas, USA

[3]Department of Microbial Pathogenesis and Immunology, Texas A&M University, College Station, Texas, USA

Correspondence
Arum Han, Department of Electrical and Computer Engineering, Texas A&M University, College Station, TX 77843, USA.
Email: arum.han@ece.tamu.edu

Funding information
Medistar Corporation; National Institute of Allergy and Infectious Diseases, Grant/Award Number: 1R01AI141607-01A1

Abstract

Heat treatment denatures viral proteins that comprise the virion, making the virus incapable of infecting a host. Coronavirus (CoV) virions contain single-stranded RNA genomes with a lipid envelope and four proteins, three of which are associated with the lipid envelope and thus are thought to be easily denatured by heat or surfactant-type chemicals. Prior studies have shown that a temperature as low as 75°C with a treatment duration of 15 min can effectively inactivate CoV. The degree of CoV heat inactivation greatly depends on the length of heat treatment time and the temperature applied. With the goal of finding whether sub-second heat exposure of CoV can sufficiently inactivate CoV, we designed and developed a simple fluidic system that can measure sub-second heat inactivation of CoV. The system is composed of a stainless-steel capillary immersed in a temperature-controlled oil bath followed by an ice bath, through which virus solution can flow at various speeds. Flowing virus solution at different speeds, along with temperature control and monitoring system, allows the virus to be exposed to the desired temperature and treatment durations with high accuracy. Using mouse hepatitis virus, a betacoronavirus, as a model CoV system, we identified that 71.8°C for 0.51 s exposure is sufficient to obtain >5 Log_{10} reduction in viral titer (starting titer: 5×10^7 PFU/ml), and that when exposed to 83.4°C for 1.03 s, the virus was completely inactivated (>6 Log_{10} reduction).

KEYWORDS
coronavirus, COVID-19, heat inactivation of coronavirus, SARS-CoV-2, sub-second virus disinfection

1 | INTRODUCTION

Severe acute respiratory syndrome coronavirus 2 (SARS-CoV-2) is the virus responsible for the currently ongoing global pandemic, the coronavirus disease of 2019 (COVID-19; Lai et al., 2020; Valencia, 2020; Velavan & Meyer, 2020). The main transmission routes of SARS-CoV-2 include direct or indirect contact with objects or contaminated surfaces, short-range person-to-person transmission via droplets from coughing or sneezing, and long-range airborne transmission via aerosols (Morawska & Cao, 2020). Therefore, environmental sterilization and virus inactivation are of great importance to prevent and control the spread of the virus. Currently, the most commonly used methods to sterilize or inactivate viruses include treatments using chemical agents, UV irradiation exposure, and heat treatment, which have been intensively assessed and reported (Darnell et al., 2004; Heilingloh et al., 2020; Inagaki et al., 2020; Kratzel et al., 2020; Pastorino et al., 2020;

Yuqian Jiang and Han Zhang contributed equally to this study.

Ratnesar-Shumate et al., 2020). Compared with other methods, one major advantage of heat treatment is its relatively shorter treatment time and simplistic method, along with the ability to be incorporated into various human-occupied spaces (Batéjat et al., 2021; Kariwa et al., 2006; Yap et al., 2020). These features allow for such heat treatment methods to be readily implemented into a variety of existing applications or systems that could be retrofitted to add rapid pathogen inactivation functionality, such as to existing heating, ventilation, and air conditioning (HVAC) systems as well as sewer systems.

Heat inactivation is a relatively easy, safe, and efficient method to disinfect coronavirus (CoV), as CoV is an enveloped virus that is surrounded by a lipid bilayer with viral spike proteins projecting from the lipid envelope, where both the envelope and the spike protein are susceptible to heat (Schoeman & Fielding, 2019). Previous studies have shown that at a temperature of 56°C and higher, with heat application time typically longer than 1 min, is needed to efficiently inactivate CoVs such as SARS-CoV and MERS-CoV (>6 Log_{10} reduction; Darnell et al., 2004; Pastorino et al., 2020; Yap et al., 2020). More specifically, at relatively low temperatures (56–65°C), treatment time of 15–60 min were required, while at higher temperatures (70–100°C) a much shorter duration of 1–15 min were needed (Chin et al., 2020; Darnell et al., 2004; Leclercq et al., 2014; Pastorino et al., 2020; Saknimit et al., 1988; Yap et al., 2020). For example, heat treatment of SARS-CoV-2 at 70°C for 5 min achieved >4.5 Log_{10} reduction (Chin et al., 2020), with another study reported that heat treatment at 92°C for 15 min achieved >6 Log_{10} reduction for SARS-CoV-2 (Pastorino et al., 2020). However, for heat treatment to be utilized for liquid and airborne CoV inactivation in broad ranges of practical settings, such methods need to be applicable at a significantly shorter heat treatment time (even if the temperature itself has to be much higher). Otherwise, there is limited practicality in such heat treatment methods. For example, having to increase the temperature of liquid for minutes would consume a large amount of energy, and having to treat air for minutes is impractical.

Here, we hypothesize that a much shorter heat treatment time may be sufficient to destroy key components of CoVs (e.g., envelope or the spike proteins) to inactivate CoV. Conventional testing methods for the heat treatment of CoVs mostly utilize a simple method of dipping a CoV-containing tube into a temperature-controlled water bath. Such methods are valid when heat treatment time in the range of minutes is tested but cannot be used for seconds or sub-second testing. In this study, we developed a simple flow-through heating and cooling method utilizing a stainless-steel capillary tube and used the method to investigate the effect of CoV heat treatment at an extremely short heat exposure time of 0.1–1 s (equivalent to actual treatment time of 0.18–2.30 s, obtained through heat transfer simulation) at an actually applied temperature range of 35–100°C. This study provides essential data for the development of sub-second CoV heat inactivation approaches, including methods to efficiently inactivate airborne CoVs indoors. As all CoVs are surrounded by lipid bilayer membranes with similar proteins and have similar physical properties (Schoeman & Fielding, 2019), we expect that our findings using mouse hepatitis virus (MHV), a betacoronavirus, as a model system that has extensively used as a surrogate coronavirus (Casanova et al., 2009; Hulkower et al., 2011; Körner et al., 2020;

Ye et al., 2016), can be broadly applicable to CoVs in general, including SARS-CoV, SARS-CoV-2, and MERS-CoV, to name a few. One of the potential applications of our findings is to heat inactivate airborne viruses by renovating a ventilation system, and another promising application is to disinfect the sewer system by scaling up the presented system and optimizing the system design. A previous study showed that the time needed for SARS-CoV-2 inactivation can be reduced to 5 min when the treatment temperature is 70°C (Chin et al., 2020). Taking consideration of our findings, if a filter in an HVAC system can be heated to a high temperature, SARS-CoV-2 in the circulating air can be efficiently killed rapidly. Here, the needed temperature to completely (or mostly) inactivate the viruses can be determined based on our data. Since many other viruses, such as dengue virus, influenza virus, and measles virus, are also enveloped viruses where the envelopes contain surface proteins (Gelderblom, 1996), we expect that this heat inactivation method can have broad utility in inactivating/disinfecting many other viruses of global consequences.

2 | MATERIALS AND METHODS

2.1 | Virus and cells preparation

The coronavirus used in this study is mouse hepatitis virus strain A59 (MHV-A59) and has been described previously (Bond et al., 1979; Wippold et al., 2020). Mouse L2 cells, which are susceptible to MHV infection, were grown in Dulbecco's modified Eagle's medium (DMEM) supplemented with 4 mM glutamine and 10% defined calf serum (Hyclone) at 37°C 5% CO_2 environment (Sturman & Takemoto, 1972).

2.2 | Virus titration and plaque assay

Plaque assays were conducted as described previously, and viral titer quantified at 2 days postinfection after removing the agarose overlay and staining the cells with crystal violet (Leibowitz et al., 2011). Samples were assayed in triplicate and the number of plaques was counted. Infectivity was determined and expressed as plaque-forming units (PFUs) per ml.

2.3 | Heat treatment of virus solution

Figure 1 shows the experimental setup that allows rapid and high-temperature heat treatment of viruses. A stainless-steel (SS) capillary tubing (SS 304, 1/16 in. outer diameter [1572 μm], 0.02 in. [500 μm] wall thickness, 0.0225 in. [572 μm] inner diameter, Mcmaster-Carr) was bent and immersed in an oil bath and then in an ice bath sequentially. A relatively small inner diameter tubing was selected to minimize the volume of the solution so that the virus solution can be rapidly heated and cooled down. SS was utilized to maximize heat conduction from the exterior to the interior of the tubing. Since a short pulse of the high-temperature application was desired to
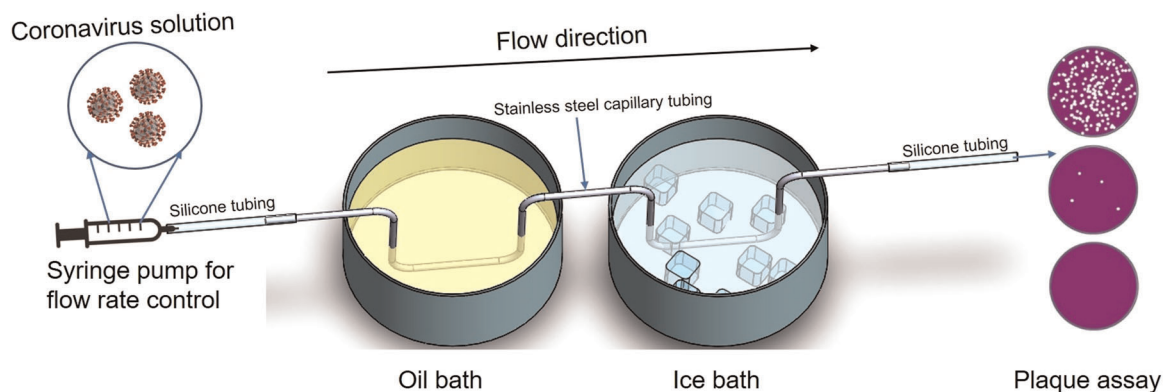
FIGURE 1 Schematic illustration of the virus heat inactivation testing system [Color figure can be viewed at wileyonlinelibrary.com]

accurately assess the impact of the temperature on viral infectivity, an ice bath was utilized to rapidly cool down the heated viral solution. A temperature-controlled oil bath (Instatherm® Economy Bath/Controller Kit, Ace Glass, Inc., VWR) equipped with a Type J thermocouple temperature sensor was employed to control the heat treatment temperature. Vegetable cooking oil (Member's mark, Sam's Club) was used in the oil bath. A mixture of ice and water was used as the ice bath to cool down the treated virus solution immediately after treatment. A syringe pump (Fusion 200, Chemyx) was employed to control the flow rate of the injected virus solution. Silicone tubing was used to connect the syringe to the inlet of the SS tubing and also to collect the heat-treated samples from the outlet of the SS tubing. Low-thermal-conducting silicone tubing was utilized to further limit the temperature exposure to only a short section of the overall tubing. The collected virus samples were stored at −80°C until plaque assays were conducted to measure the infectivity of the heat-treated viruses.

Stock MHV viruses of 2.7×10^9 PFU/ml were diluted by DMEM media with 10% FBS to 5×10^7 PFU/ml, a high-enough titer to accurately determine the effectiveness of heat treatment on viral infectivity. For each heat treatment, a virus solution aliquot of 1.5 ml containing approximately 75 million viral PFUs was injected into the SS capillary tubing under varying flow rates by a syringe pump while the oil bath temperature was set to 55–170°C. The heat-treated samples were collected at the outlet of the silicone tubing. The set exposure time was calculated based on the traveling distance of the viral solution through the length of the SS tubing immersed in the oil bath (5 cm). The flow rate and set exposure time are summarized in Table S1. A viral solution flowing through the tubing while the oil bath temperature was set to room temperature (22°C) was used as a control to account for any potential viral titer reduction due to virus adhering to the tubing surfaces and other potential losses.

2.4 | COMSOL simulation of temperature

The COMSOL Multiphysics 5.5a software (COMSOL Inc.) was used for the temperature profile simulation of the viral solution.

To perform this finite element analysis, a 3D geometry was chosen, where the geometry was created using the following initial and boundary conditions (Zhang et al., 2019, 2020): no-slip conditions on the tubing surfaces; the fluid is Newtonian and the flow within the channel is incompressible; no viscous stress and convective flux on the tubing outlet; convective heat flux is considered as the source of heat influx from the oil to the tubing.

The simulation was performed using non-isothermal flow (nitf) multi-physical interfaces laminar flow (spf) coupled with heat transfer in solids and fluids (ht) under the stationary study model. The initial inlet flow temperature and ambient air temperature were set to 22°C. The material physical properties of viral solution were set to be identical to those of water. The material properties of the SS tubing were set to: density = 7850 kg/m^3; thermal conductivity = 16.2 W/(m K); heat capacity at constant pressure = 500 J/(kg K). Here, we assume the overall heat loss by the oil bath is equal to the overall heat gain of water flowing by (the heat loss to ambient air is deemed negligible). Then, the temperature-dependent heat transfer coefficient (H) was calculated based on Equation (1) (Bergman et al., 2011; Shashi Menon, 2015) and the real-time temperature measurement (see Section 2.5 for more details). The calculated H value is 473.6 W/(m^2 K) under the thermal treatment condition of 125°C (oil bath temperature) for 0.5 s (based on the length of merged SS tubing and set flow rate), while the H value increased to 675.5 W/(m^2 K) when the treatment condition is 170°C for 0.1 s. The H values obtained in this study are close to previously published results (Kobasko et al., 2010). Physics-controlled mesh with the element size of "finer" was applied for the simulation. A mesh refinement testing using the typical condition of 125°C and 0.5 s exposure time was conducted (Figure S1). The mesh convergence test result (see Figure S1 for more details) indicates the mesh is refined enough to obtain a solution that can be trusted (the relative error is 2%–3% when compared to the "finer" mesh result with the threshold value, where the convergent value at "extremely fine" mesh condition was used as threshold value).

$$H \times A \times (T_{oil} - T_{ss}) = C_w \times Q_w \times \rho \times (T_{in} - T_{out}) \quad (1)$$

where

A: surface area where the heat transfer takes place;

T_{oil}: temperature of the surrounding oil;

T_{ss}: temperature of the solid surface;

C_w: heat capacity of water;

Q_w: flow rate of water;

ρ: density of water;

T_{in}: water temperature at inlet; and

T_{out}: water temperature at outlet.

2.5 | Real-time temperature measurement and validation of the measurement method

To measure the real-time temperature of the viral solution flowing through the tubing while the heat is applied through the heated oil bath, the SS tubing was cut apart between the oil bath and the ice bath, and the two ends were re-connected through a T-connector with an insulation material (Fiberglass) wrapped around the connector (Mcmaster-carr). A J-type thermocouple was inserted through the top end of the T-connector to obtain the real-time temperature of the viral solution flowing through the tubing. The temperature of the tubing wall was measured by attaching the sensor head of the thermocouple to the outside wall of the SS tubing and wrapped with fiberglass.

The temperature measured by this experimental setup (T-thermocouple) was validated and calibrated by withdrawing water heated to a known temperature via a syringe pump (EGATO® 111, KD Scientific) while the temperature reading of the sensor was recorded. The schematic illustration of this measurement setup is described in Figure S2a.

3 | RESULTS AND DISCUSSION

3.1 | Validation of the viral solution treatment temperature

As our study aims to inactivate CoVs with a sub-second exposure to high temperature, accurately measuring the real temperature applied to the viral solution is imperative. Since the solution cannot be heated up or cooled down instantaneously and the desired temperature exposure time is quite short, this is nontrivial. First, to validate whether the thermocouple inserted into the T-junction of the SS tubing (called T-thermocouple here) can accurately measure the solution temperature inside the SS tubing, a solution with known temperature, set by heating the bulk of the solution in a temperature-controlled water bath, was drawn into the SS tubing at various flow speeds and its temperature was measured. This measured temperature inside the SS tubing (2 cm away from the heated water bath) was then compared to that of the bulk solution temperature. Figure S2b shows these calibration curves. The results show that the temperature probe accurately measures the solution temperature inside the SS tubing. For example, at a fast flow of 0.1 s

exposure, which minimizes any cooling of the solution outside of the water bath, the measured temperature was almost identical to the water bath temperature (Figure S2b, 0.1 s condition, 97.8°C water bath temperature = 97.7°C measured temperature). Second, when the flow rate was set lower (i.e., longer exposure to ambient temperature), it is expected that the solution will cool down slightly the moment it leaves the SS tubing section immersed inside the water bath. Indeed, the measurement result shows that as the treatment time increases to 0.25, 0.5, and 1 s (i.e., slower flow rate), the measured temperature becomes slightly lower than the water bath temperature. For example, for water bath temperature of 98.0°C and exposure time of 0.25, 0.5, and 1 s, the T-thermocouple temperature readings were 95.4, 94.5, and 92.6°C, showing slight cooling of the solution flowing inside the tubing. Therefore, the actual temperature of the virus solution was corrected by the calibration curves (Figure S2b), which were then used as the actual temperatures virus solution was exposed to.

3.2 | COMSOL heat transfer simulation

The heat transfer efficiency and temperature profile within the SS capillary tubing are important to understand the actual heating condition of the viral solution. We used COMSOL Multiphysics™ to simulate the heat transfer from the SS tubing to the flowing CoV solution inside the tubing. The experiments were conducted at steady state, and thus there is no transient term. The maximum Reynolds number is approximately 520 obtained from the condition of 0.5 m/s and applied oil bath temperature of 160°C (real solution temperature inside the tubing measured was 56°C), which is much lower than the critical Reynold number of 2300 for turbulence flow. In this laminar flow regime, we anticipate a temperature gradient along the radial direction of the pipe. At steady state, the temperature gradient does not change with time, but is a function of the location along the axial direction. Figure 2a shows the temperature change of flowing virus solution within the SS tubing when the oil bath temperature was set to 125°C and a moderate exposure time of 0.5 s (flow rate = 92,300 µl/h) was used. Here, the SS tubing temperature increases rapidly as it enters the oil bath (pink zone), then gradually drops when the tubing is exposed to air (yellow zone), and then rapidly drops as it enters the ice bath (blue zone). The reason that the SS temperature inside the oil bath (pink zone) is not the same as the oil bath temperature is due to the cooling effect of room temperature virus solution continuously flowing into the tubing, especially since the length of the tubing immersed inside the oil bath was relatively short (5 cm). Using a much longer tubing inside the oil bath would have eventually made the SS tubing temperature the same as the oil bath temperature, but that makes it impossible to apply a short heat exposure, the reason why a relatively short tubing length was utilized.

The virus solution temperature follows the SS tubing temperature relatively closely. The highest solution temperature of 85.9°C was achieved right as it comes out from the oil bath (this highest
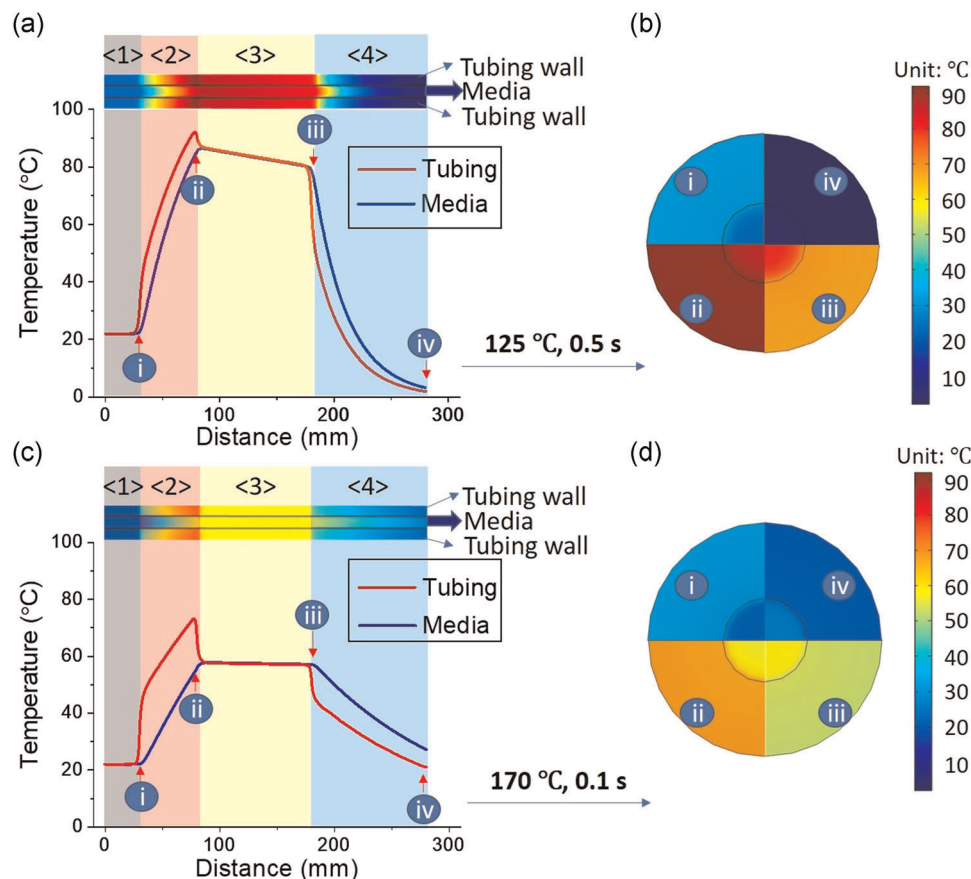
FIGURE 2 The simulated temperature distribution of the entire heat inactivation testing system when using the oil bath to apply heat. The top color bar represents the axial cross-sectional SS tubing, and traverse sectional views of positions i–iv are displayed in the right circles. (a) 125°C, 0.5 s exposure condition, along with the (b) corresponding traverse sectional views. (c) 170°C, 0.1 s exposure condition, along with the (d) corresponding traverse sectional view. Zone <1> pre-oil bath; Zone <2> oil bath; Zone <3> ambient air; Zone <4> ice bath. The distance for simulation starts from 30 mm before the oil bath [Color figure can be viewed at wileyonlinelibrary.com]

temperature is referred to as the simulated temperature (Max) in Table S1) and maintains its temperature relatively stable (temperature drop of only 6.5°C over a 10 cm length), until arriving at the segment of the SS tubing immersed in the ice bath. Therefore, the effective heat treatment region was designated from the temperature point within the oil bath (pink zone) where the temperature rises above that of the pre-ice bath temperature (the ending temperature of the yellow zone) to the pre-ice bath temperature. The "actual exposure time" was calculated based on this "effective heat treatment region" (the length is slightly longer than 10.0 cm). For example, in the case of 125°C 0.5 s heat treatment condition, this "actual exposure time" is around two times longer than the set exposure time, which in this case was 1.03 s.

Figure 2c exhibits the temperature distribution under the condition of 170°C oil bath temperature and "set exposure time" of 0.1 s (flow rate = 461,500 μl/h). Even though the set temperature was higher, due to the five times faster flow rate of incoming room temperature solution, the SS tubing temperature only reached a peak value of around 72°C due to the larger cooling effect coming from the incoming solution (for the 125°C, 0.5 s condition, the SS tubing reached a temperature around 92°C). This effect can also be seen by

the drop in the SS tubing temperature as it exits the oil bath. In this case, the highest solution temperature of 58.1°C was at the point where the SS tubing exits the oil bath, with a minimum drop in temperature until it enters the ice bath. Thus, as before, the effective heat treatment region could be designated similarly. The temperature comparison table summarizes (Table S1) the set oil bath temperature, the calibrated real-time temperature based on the T-junction temperature sensor readout, and the actual temperature that accommodates the cooling effect.

3.3 | Heat inactivation of MHV

An average viral load of SARS-CoV-2 is 7×10^6 per ml (Stadnytskyi et al., 2020), therefore we chose 5×10^7 PFU/ml of MHV, which is a slightly higher concentration and would also provide a rigorous test for the rapid heat inactivation system presented here. Our study investigated the effect of rapid heat treatment (<1 s) on coronavirus inactivation by flowing the MHV virus solution through a stainless tubing immersed in an oil bath, which temperature was controlled from 55 to 170°C. We found that the coronavirus was inactivated

efficiently (>6 Log_{10} reduction) by applying an oil bath temperature of 115°C and residence time of 1 s (set exposure time). When the set exposure time decreased to 0.5 s, an oil bath set the temperature of 125°C (actual temperature = 83.4°C) or higher was needed to completely inactivate the MHV. When the set exposure time further decreased to 0.25 s, the virus titer reduction was >6 Log_{10} at an oil bath set the temperature of 150°C (actual temperature = 81.3°C). However, when the set exposure time was reduced to 0.1 s, MHV could not be sufficiently inactivated even when the oil bath set temperature was increased to 170°C (Figure 3a).

These results were then re-plotted based on the actual treatment temperature and exposure time, as shown in Figure 3b. As discussed in Section 3.2, the actual exposure time calculated was around two times longer than the set exposure time. For visualization purposes, the actual exposure times were rounded to 2, 1, 0.5, and 0.2 s (Table S1, the temperature ranges for the rounding were 2.01–2.30, 0.98–1.07, 0.48–0.54, and 0.18–0.2 s, respectively), which are corresponding to the set exposure time of 1, 0.5, 0.25, and 0.1 s. Among the oil bath set temperatures ranging from 55 to 170°C, the

shortest treatment time required to inactivate the MHV effectively (>5 Log_{10} reduction) was concluded as 0.25 s set exposure time (0.51 s actual exposure time), with an actual exposure temperature of 71.8°C (oil bath set temperature = 140°C). However, when the oil bath set temperature was increased to 150, 160, and 170°C, slightly higher remaining virus titers (mean values) were obtained with relatively large error bars (three to five repeats). Furthermore, among the oil bath set temperature we tested (55–170°C), the most rapid thermal treatment to completely inactivate MHV (>6 Log_{10} reduction with the remaining viral titer = 0 PFU/ml) was determined to be 0.5 s set exposure time (1.03 s actual exposure time), with an actual exposure temperature of 83.4°C (oil bath set temperature = 125°C). When these results were plotted into a 2D format (Figure S3b), the correlation between the viral inactivation and actual exposure temperature showed that heat treatment temperature as high as around 70°C is required to effectively provide sub-second heat inactivation (>5 Log_{10} reduction) regardless of the actual treatment time.

Table 1 summarizes the inactivation effectiveness under different heat treatment conditions, where our results were highlighted
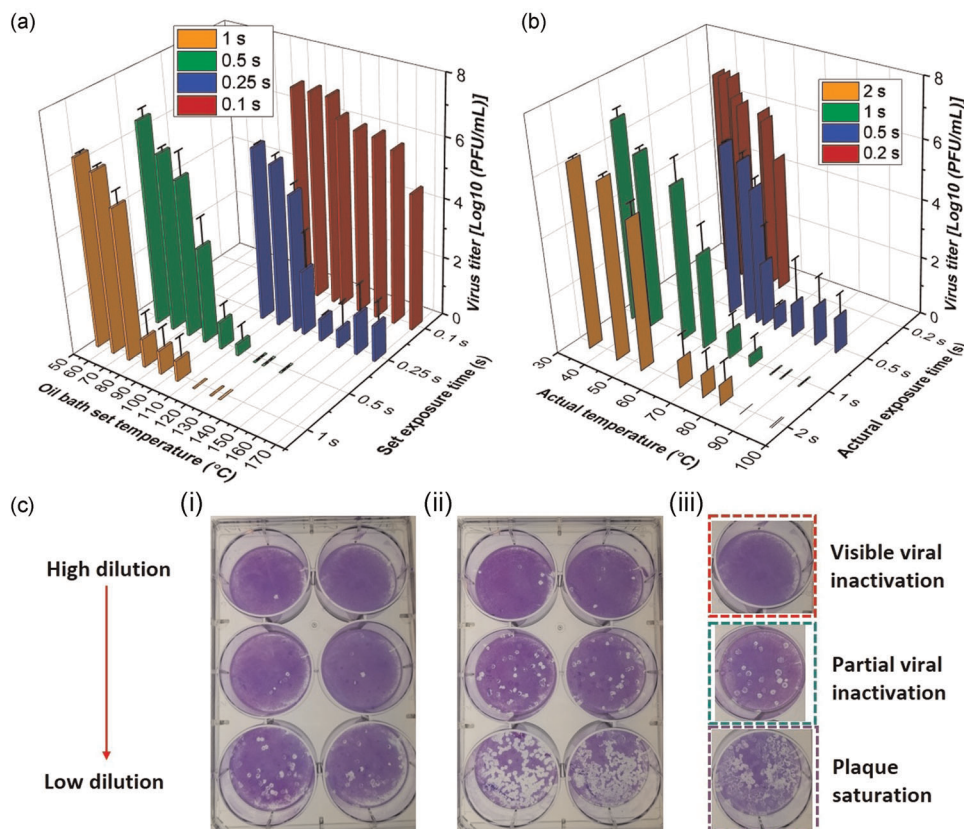

FIGURE 3 Effect of heat treatment on the infectivity of MHV. Remaining infectivity of MHV after different heat inactivation conditions (a) by oil bath set temperature and set exposure time; (b) by actual exposure temperature from real-time measurement and actual exposure time based on simulation. Virus titers were averaged from three independent biological replicates (n = 3), and error bars indicate standard deviations. (c) Example images from the quantitative plaque assay that was used to determine posttreatment PFUs of the MHVs: (i) No plaque formation at high dilution but several plaques formed at low dilution indicates remaining infectivity of MHV; (ii) Examples of wells with too many plaques indicate large amount of infection-capable MHVs, which require a further dilution to accurately conduct plaque count; (iii) Examples of plaque assay result after successful MHV heat inactivation (no plaque formation even at original "no diluted" sample solution, top red box), unsuccessful heat inactivation (or partial inactivation depending on its dilution; middle green box), and assays that need to be repeated at higher dilution for accurate plaque count (bottom purple box) [Color figure can be viewed at wileyonlinelibrary.com]

TABLE 1 Summary of previously reported heat inactivation conditions with temperature ranging from room temperature to 120°C for heating duration from sub-second to 1 h

#	Temperature (°C)	Exposure duration	Remaining infectivity	Log_{10} reduction	Virus type	Other notes	References
1	22–25	7 days		1.5–2	SARS CoV	RH 40%–50%	Chan et al. (2011)
2	22–25	28 days		>5	SARS CoV	RH 40%–50%	Chan et al. (2011)
3	40	1 min		0.16	MHV-2		Saknimit et al. (1988)
4	40	5 min		0.33	MHV-2		Saknimit et al. (1988)
5	40	15 min		0.34	MHV-2		Saknimit et al. (1988)
6	42	60 min		<1	SARS-CoV-2		Wang et al. (2020)
7	56	1 min	6.65		SARS-CoV-2		Chin et al. (2020)
8	56	15 min		4.92	MERS-CoV		Leclercq et al. (2014)
9	56	15 min		3–4	SARS-CoV-2		Wang et al. (2020)
10	56	20 min	Incompletely inactivated	>5	SARS-CoV		Darnell et al. (2004)
11	56	30 min	Incompletely inactivated	>5	SARS-CoV-2		Pastorino et al. (2020)
12	56	30 min	ND	>4.51	SARS-CoV-2		Chin et al. (2020)
13	60	1 min		2.60	MHV-2		Saknimit et al. (1988)
14	60	5 min		3.55	MHV-2		Saknimit et al. (1988)
15	60	10 min		>6	SARS-CoV-1	Model prediction	Yap et al. (2020)
16	60	15 min		>4.51	MHV-2		Saknimit et al. (1988)
17	60	15 min	ND	>7	SARS-CoV-2		Wang et al. (2020)
18	60	30 min		>4.51	MHV-2		Saknimit et al. (1988)
19	60	60 min	Incompletely inactivated	>5	SARS-CoV-2		Pastorino et al. (2020)
20	60.2	0.20 s		>2	MHV		This study
21	65	30 s		3.45	MERS-CoV		Leclercq et al. (2014)
22	65	1 min	Incompletely inactivated	Data not shown	MERS-CoV		Leclercq et al. (2014)
23	65	4 min	Incompletely inactivated	>5	SARS-CoV		Darnell et al. (2004)
24	65	15 min	ND	>5.59	MERS-CoV		Leclercq et al. (2014)
25	70	1 min	5.34	~1.25	SARS-CoV-2		Chin et al. (2020)
26	70	5 min	ND	>4.5	SARS-CoV-2		Chin et al. (2020)
27	71.8	0.51 s		>5	MHV		This study
28	75	15 min	ND	>5	SARS-CoV		Darnell et al. (2004)
29	80	<1 min		>6	SARS-CoV-1	Model prediction	Yap et al. (2020)
30	80	1 min		>4.51	MHV-2		Saknimit et al. (1988)
31	83.4	1.03 s	ND	>6	MHV		This study
32	87.3	2.23 s	ND	>6	MHV		This study
33	90	0.1 min		6	MERS-CoV	Model prediction	Yap et al. (2020)
34	92	15 min	ND	>6	SARS-CoV-2		Pastorino et al. (2020)
35	110	0.1 min		6	SARS-CoV-1	Model prediction	Darnell et al. (2004)
36	112	0.01 min		6	MERS-CoV	Model prediction	Darnell et al. (2004)
37	120	~1 s		6	SARS-CoV-1	Model prediction	Kratzel et al. (2020)

Abbreviation: ND, not detectable.

with shade. In general, coronaviruses are relatively stable at room temperature and are sensitive to heat when the temperature increased to 65°C, after which the degree of inactivation linked to temperature became obvious. Since a small increase in temperature (after 65°C) results in a large increase in inactivation percentage and the temperature experienced by the viruses are not equal to the applied heating temperature (Abraham et al., 2020), our study fills a gap of sub-second heat treatment.

4 | DISCUSSION AND CONCLUSION

We developed an experimental system and protocol that can conduct sub-second thermal treatment of coronaviruses, identified the thermal treatment conditions that result in efficient thermal inactivation of coronaviruses. We successfully developed an experimental setup that allows applying sub-second duration of heat to coronavirus solution where the temperature applied to the CoV solution can be monitored in real time. Through experimental measurement and computational thermal simulation, we validated the real temperature that the CoV solutions are exposed to. Using this setup and MHV (a model betacoronavirus), we identified that applying a temperature of 71.8°C (actual temperature) for 0.51 s (actual exposure time) is sufficient to obtain >5 Log_{10} reduction in viral titer (starting titer: 5×10^7 PFU/ml), and that when exposed to 83.4°C (actual temperature) for 1.03 s (actual exposure time), the virus was completely inactivated (zero titer, >6 Log_{10} reduction). This is the first systematic study on how very short heat treatment time at various temperatures influences viral infectivity, through which we have identified for the first time the minimum temperature and exposure time required to inactive the infectivity of CoV. The previous study by Yu et al., where direct heat inactivation of airborne viruses at 200°C was demonstrated, indeed shows that sub-second exposure is sufficient to inactivate viruses. Our result presented here can provide critical information to such systems where a significantly lower temperature than the tested 200°C in their study may be sufficient to heat-inactivate CoV. Considering other examples and conditions such as hospital operation rooms, where the airflow rate is much faster (around 0.15–0.18 m/s; Khankari, 2018; Memarzadeh & Manning, 2002), our study results can provide important design criteria such as how thick a heat-applying filter has to be to provide sufficient treatment time. Of course, to apply CoV inactivation strategies in any practical applications, confirmation experiments have to be conducted with the authentic CoV of interest. Since heat treatment is a simple, inexpensive, and efficient approach to inactivate coronaviruses, our method can be used to further study the thermal sensitivity of viruses, as well as providing critical data that can be used to develop efficient CoV heat inactivation methods that can be broadly applied to real-world settings.

AUTHOR CONTRIBUTIONS

Arum Han, Yuqian Jiang, Han Zhang, and Jose A. Wippold conceived and designed the experiments. Yuqian Jiang performed the heat inactivation experiments and data analysis. Han Zhang performed the simulation and related data acquisition. Jyotsana Gupta performed cell culture and the virus titer plaque assays. Jose A. Wippold contributed to the original experimental setup and Jing Dai set up the temperature validation device. Arum Han, Paul de Figueiredo, and Julian L. Leibowitz participated in critical revision of the manuscript and other intellectual contributions. Yuqian Jiang and Han Zhang wrote and revised the majority of the manuscript, with all authors contributing to the preparation of the manuscript.

ORCID

Yuqian Jiang [ID] http://orcid.org/0000-0001-8580-2018

REFERENCES

Abraham, J. P., Plourde, B. D., & Cheng, L. (2020). Using heat to kill SARS-CoV-2. *Reviews in Medical Virology*, e2115.

Batéjat, C., Grassin, Q., Manuguerra, J.-C., & Leclercq, I. (2021). Heat inactivation of the severe acute respiratory syndrome coronavirus 2. *Journal of Biosafety and Biosecurity*, *3*(1), 1–3.

Bergman, T. L., Incropera, F. P., DeWitt, D. P., & Lavine, A. S. (2011). *Fundamentals of heat and mass transfer*. John Wiley & Sons.

Bond, C. W., Leibowitz, J. L., & Robb, J. A. (1979). Pathogenic murine coronaviruses II. Characterization of virus-specific intracellular proteins of JHMV and A59V. *Virology*, *94*, 371–384.

Casanova, L., Rutala, W. A., Weber, D. J., & Sobsey, M. D. (2009). Survival of surrogate coronaviruses in water. *Water Research*, *43*(7), 1893–1898.

Chan, K.-H., Peiris, J. M., Lam, S., Poon, L., Yuen, K., & Seto, W. H. (2011). The effects of temperature and relative humidity on the viability of the SARS coronavirus. *Advances in Virology*, *2011*, 1–7.

Chin, A. W. H., Chu, J. T. S., Perera, M. R. A., Hui, K. P. Y., Yen, H.-L., Chan, M. C. W., Peiris, M., & Poon, L. L. M. (2020). Stability of SARS-CoV-2 in different environmental conditions. *The Lancet Microbe*, *1*(1), e10. https://doi.org/10.1016/S2666-5247(20)30003-3

Darnell, M. E., Subbarao, K., Feinstone, S. M., & Taylor, D. R. (2004). Inactivation of the coronavirus that induces severe acute respiratory syndrome, SARS-CoV. *Journal of Virological Methods*, *121*(1), 85–91.

Gelderblom, H. R. (1996). Structure and classification of viruses, *Medical microbiology* (4th ed.). University of Texas Medical Branch.

Heilingloh, C. S., Aufderhorst, U. W., Schipper, L., Dittmer, U., Witzke, O., Yang, D., Zheng, X., Sutter, K., Trilling, M., Alt, M., Steinmann, E., & Krawczyk, A. (2020). Susceptibility of SARS-CoV-2 to UV irradiation. *American Journal of Infection Control*, *48*, 1273–1275.

Hulkower, R. L., Casanova, L. M., Rutala, W. A., Weber, D. J., & Sobsey, M. D. (2011). Inactivation of surrogate coronaviruses on hard surfaces by health care germicides. *American Journal of Infection Control*, *39*(5), 401–407.

Inagaki, H., Saito, A., Sugiyama, H., Okabayashi, T., & Fujimoto, S. (2020). Rapid inactivation of SARS-CoV-2 with deep-UV LED irradiation. *bioRxiv*.

Kariwa, H., Fujii, N., & Takashima, I. (2006). Inactivation of SARS coronavirus by means of povidone-iodine, physical conditions and chemical reagents. *Dermatology, 212*(Suppl 1), 119–123.

Khankari, K. (2018). Hospital operating room ventilation systems. *ASHRAE Journal, 60*(6), 16–26.

Kobasko, N. I., de Souza, E. C., de Compos Franceschini Canale, L., & Totten, G. E. (2010). Vegetable oil quenchants: Calculation and comparison of the cooling properties of a series of vegetable oils. *Strojniski Vestnik/Journal of Mechanical Engineering, 56*(2).

Kratzel, A., Todt, D., V'kovski, P., Steiner, S., Gultom, M., Thao, T. T. N., Ebert, N., Holwerda, M., Steinmann, J., Niemeyer, D., Dijkman, R., Kampf, G., Drosten, C., Steinmann, E., Thiel, V., & Pfaender, S. (2020). Inactivation of severe acute respiratory syndrome coronavirus 2 by WHO-recommended hand rub formulations and alcohols. *Emerging Infectious Diseases, 26*(7), 1592–1595.

Körner, R. W., Majjouti, M., Alcazar, M. A. A., & Mahabir, E. (2020). Of mice and men: The coronavirus MHV and mouse models as a translational approach to understand SARS-CoV-2. *Viruses, 12*(8), 880.

Lai, C.-C., Shih, T.-P., Ko, W.-C., Tang, H.-J., & Hsueh, P.-R. (2020). Severe acute respiratory syndrome coronavirus 2 (SARS-CoV-2) and coronavirus disease-2019 (COVID-19): The epidemic and the challenges. *International Journal of Antimicrobial Agents, 55*, 105924.

Leclercq, I., Batejat, C., Burguière, A. M., & Manuguerra, J. C. (2014). Heat inactivation of the Middle East respiratory syndrome coronavirus. *Influenza and Other Respiratory Viruses, 8*(5), 585–586.

Leibowitz, J., Kaufman, G., & Liu, P. (2011). Coronaviruses: Propagation, quantification, storage, and construction of recombinant mouse hepatitis virus. *Current Protocols in Microbiology, 15*(1), 15E.1.1–15E.1.46. https://doi.org/10.1002/9780471729259.mc15e01s21

Memarzadeh, F., & Manning, A. P. (2002). Comparison of operating room ventilation systems in the protection of the surgical site/discussion. *ASHRAE Transactions, 108*, 3.

Morawska, L., & Cao, J. (2020). Airborne transmission of SARS-CoV-2: The world should face the reality. *Environment International, 139*, 105730.

Pastorino, B., Touret, F., Gilles, M., De Lamballerie, X., & Charrel, R. N. (2020). Evaluation of heating and chemical protocols for inactivating SARS-CoV-2. *Viruses, 12*(624), 1–6.

Ratnesar-Shumate, S., Williams, G., Green, B., Krause, M., Holland, B., Wood, S., Bohannon, J., Boydston, J., Freeburger, D., Hooper, I., Beck, K., Yeager, J., Altamura, L. A., Biryukov, J., Yolitz, J., Schuit, M., Wahl, V., Hevey, M., & Dabisch, P. (2020). Simulated sunlight rapidly inactivates SARS-CoV-2 on surfaces. *The Journal of Infectious Diseases, 222*, 214–222.

Saknimit, M., Inatsuki, I., Sugiyama, Y., & Yagami, K.-i. (1988). Virucidal efficacy of physico-chemical treatments against coronaviruses and parvoviruses of laboratory animals. *Experimental Animals, 37*(3), 341–345.

Schoeman, D., & Fielding, B. C. (2019). Coronavirus envelope protein: Current knowledge. *Virology Journal, 16*(1), 1–22.

Shashi Menon, E. (2015). Thermal hydraulics. In E. Shashi Menon (Ed.), *Transmission pipeline calculations and simulations manual* (pp. 273–316). Gulf Professional Publishing.

Stadnytskyi, V., Bax, C. E., Bax, A., & Anfinrud, P. (2020). The airborne lifetime of small speech droplets and their potential importance in SARS-CoV-2 transmission. *Proceedings of the National Academy of Sciences of the United States of America, 117*(22), 11875–11877.

Sturman, L. S., & Takemoto, K. K. (1972). Enhanced growth of a murine coronavirus in transformed mouse cells. *Infection and Immunity, 6*, 501–507.

Valencia, D. N. (2020). Brief review on COVID-19: The 2020 pandemic caused by SARS-CoV-2. *Cureus, 12*(3).

Velavan, T. P., & Meyer, C. G. (2020). The COVID-19 epidemic. *Tropical Medicine & International Health, 25*(3), 278–280.

Wang, T., Lien, C., Liu, S., & Selveraj, P. (2020). Effective heat inactivation of SARS-CoV-2. *medRxiv*. https://www.medrxiv.org/content/10.1101/2020.04.29.20085498v1

Wippold, J. A., Wang, H., Tingling, J., Leibowitz, J. L., de Figueiredo, P., & Han, A. (2020). PRESCIENT: Platform for the rapid evaluation of antibody success using integrated microfluidics enabled technology. *Lab on a Chip, 20*(9), 1628–1638.

Yap, T. F., Liu, Z., Shveda, R. A., & Preston, D. J. (2020). A predictive model of the temperature-dependent inactivation of coronaviruses. *Applied Physics Letters, 117*(6), 060601.

Ye, Y., Ellenberg, R. M., Graham, K. E., & Wigginton, K. R. (2016). Survivability, partitioning, and recovery of enveloped viruses in untreated municipal wastewater. *Environmental Science & Technology, 50*(10), 5077–5085.

Zhang, H., Guzman, A. R., Wippold, J. A., Li, Y., Dai, J., Huang, C., & Han, A. (2020). An ultra high-efficiency droplet microfluidics platform using automatically synchronized droplet pairing and merging. *Lab on a Chip, 20*(21), 3948–3959.

Zhang, H., Zhang, W., Xiao, L., Liu, Y., Gilbertson, T. A., & Zhou, A. (2019). Use of surface-enhanced Raman scattering (SERS) probes to detect fatty acid receptor activity in a microfluidic device. *Sensors, 19*(7), 1663.

SUPPORTING INFORMATION

Additional Supporting Information may be found online in the supporting information tab for this article.